Soter, G., Garrad, M., Conn, A., Hauser, H., & Rossiter, J. (2019). Skinflow: A soft robotic skin based on fluidic transmission. In *IEEE International Conference on Soft Robotics (RoboSoft) 2019* (pp. 355-360). [8722744] Institute of Electrical and Electronics Engineers (IEEE). https://doi.org/10.1109/ROBOSOFT.2019.8722744

Peer reviewed version

License (if available):
Other

Link to published version (if available):
10.1109/ROBOSOFT.2019.8722744

Skinflow: a soft robotic skin based on fluidic transmission

Gabor Soter[1], Martin Garrad[1], Andrew T. Conn[2], Helmut Hauser[1] and Jonathan Rossiter[1]

***Abstract*— In this paper we present Skinflow, a novel soft robotic sensor based on liquid transmission. The sensor combines liquid filled soft silicone chambers and optical sensors to measure pressure, bending and vibration. When mechanically stimulated, the volume of the chambers changes and this change is transmitted to a display cell by an incompressible, coloured liquid. The displacement of the liquid in the channels is captured by a CCD camera and is quantified by image processing algorithms. We present three implementations of this concept. The first device is a soft button array with four pressure sensitive buttons. The second implementation is a three-dimensional soft touchpad, that consists of two sensor layers oriented at 90° to each other. Both layers have eight macrochannels that are filled with coloured liquid. The sensor is able to measure the position and the intensity of the touch. Finally, the third device shows how the processing unit for the proposed liquid filled sensors can be integrated using a smart vision camera and a microcontroller. Three soft bend sensors are connected to the processing unit and we control the brightness of three light emitting diodes (LEDs) in real-time by bending them. The presented sensors are safe, low cost and scalable. They can be used in soft robots, smart homes and wearables as well as for medical diagnosis, especially where electronic devices cannot be used due to electromagnetic interference (e.g. magnetic resonance imaging).**

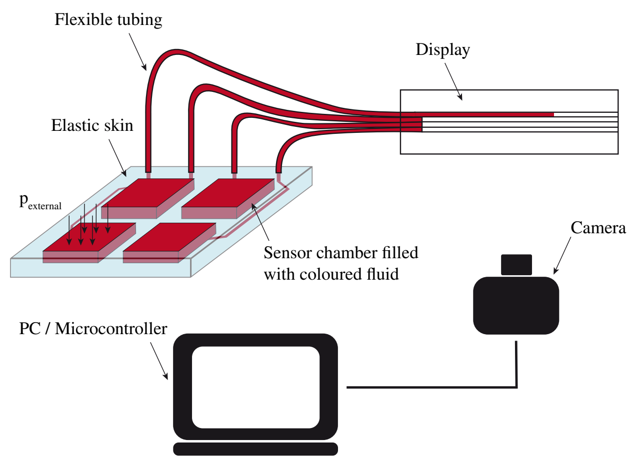

Fig. 1: The concept of the proposed sensor. Due to mechanical interaction the volume of the sensor chambers and channels embedded in the soft silicone changes and this change is transmitted by an incompressible, coloured liquid to a display. The displacement of the liquid is captured by a CCD camera and is quantified by image processing algorithms.

I. INTRODUCTION

One of the goals of soft robotics is to create robots that are lightweight, flexible and safe to use in a human environment. As they are predominantly made of soft materials it is challenging to measure their exact position and shape accurately. For this reason, soft robots often exploit different types of soft sensors that give information about the state of their body and their environment. The research on soft sensors is still in its infancy with most commonly used methods including resistive [1], capacitive [2], [3], magnetic [4], conductive liquid [5] and optical sensing [6], [7]. Here we introduce the recent developments in conductive liquid and optical based soft sensors, the most relevant to our work.

Soft sensors with conductive liquids usually include a soft silicone substrate with embedded liquid metal or ionic liquid channels. They are intrinsically stretchable, which means they can maintain conductivity during elastic deformation [8]. The most commonly used liquid metal in soft sensors is the eutectic gallium indium (eGaIn). It has excellent mechanical and electrical properties including high electrical conductivity (3.4×10^6 S/m) and low melting temperature (15° C) [9]. Many studies have reported that they can be used as pressure, force and bend sensors [8]. Manufacturing techniques for liquid metal-based soft sensors include 3D printing [10] and soft lithography [11]. However, the disadvantages of eGaIn sensors are their cost and their toxicity, which is low compared to other liquid metals (e.g. mercury), but more rigorous studies are needed to understand their impact on human health [12].

Ionic liquids are also used in compliant sensors [13]. They are cheaper and more widely available than liquid metals. However, ionic liquids have (typically three orders of magnitude) lower conductivity [14]. They can be used for actuation and sensing at the same time as they can drive the deformation of fluidic actuators as well as detect actuator deformation [15]. Recent studies investigated how liquid metals and ionic liquids can be used together in the same soft substrate [16]. The two different conductive liquids in a wearable device were applied first in [14], where the ionic liquid was used to detect strain changes and the liquid metal

[1]Gabor Soter, Martin Garrad, Helmut Hauser, and Jonathan Rossiter are with Department of Engineering Mathematics, University of Bristol, BS8 1TH, United Kingdom, and with Bristol Robotics Laboratory, BS16 1QY, United Kingdom (email:(gabor.soter, martin.garrad, helmut.hauser, jonathan.rossiter)@bristol.ac.uk.)

[2]Andrew T. Conn is with Department of Mechanical Engineering, University of Bristol, BS8 1TH, United Kingdom, and with Bristol Robotics Laboratory, BS16 1QY, United Kingdom (email: a.conn@bristol.ac.uk).

This research was partially funded by EPSRC grants EP/M026388/1, EP/P025846/1 and EP/M020460/1, EPSRC Centre for Doctoral Training in Future Robotics and Autonomous Systems (FARSCOPE) EP/L015293/1, Royal Academy of Engineering Chair in Emerging Technologies (Rossiter) and Leverhulme Trust RPG-2016-345.

microchannels were used as flexible and stretchable electrical wiring.

Optical sensors offer accurate, low cost and high resolution measurement of the large deformation of hyperelastic materials. There are many different photonic transducers that can be used as a component of soft sensors including optical fibers, light emitter diode (LED) and photodiode pairs, and CCD cameras. For example, Fiber Bragg grating sensors are extremely sensitive and can detect very small strain changes as they measure the change in reflection wavelength of an input light source. They can be integrated, for example, in robotic fingers for both force and tactile sensing [17]. Standard materials in soft robotics such as polydimethylsiloxane (PDMS) can also be used as optical waveguides; therefore a simple LED and photodiode pair between a PDMS channel can be used in a bend or strain sensor [18]. A high resolution alternative to the previous methods is offered by sensors that work with CCD cameras, such as the TacTip soft, tactile fingertip [19]. A miniature version of TacTip was integrated with a rigid robotic hand [20] and a multimodal TacTip demonstrated integrated mechano-thermal sensing [21]. A drawback of this implementation is that it is difficult to scale as a complete hand would require multiple cameras with heavy processing power.

In this paper we combine liquid filled sensors with optical sensors. The core concept is that sensory information on mechanical interaction (force, bending, vibration, etc.) can be transmitted from the place of origin to another part of the body through a non-electrical channel (see Figure 1). This way it is possible to create sensors that are soft and stretchable as well as enabling high resolution, real-time measurements and potentially high scalability. The presented method was partially inspired by fluidic actuators that mimic spider legs and have the advantage of generating the actuation force in the centre of the robot and then transmitting the actuation force to the moving arm or leg [22].

In particular, the contributions of this paper are as follows:

- To the best of our knowledge, this is the first combination of liquid transmission and optical sensing in the same device.
- We present three different sensors employing this approach: a pressure sensitive button array, a three-dimensional touchpad, and finally we present a bend sensor.
- We demonstrate how the processing can be integrated in a small unit that contains a smart vision camera and a microcontroller.

The remainder of this paper is structured as follows: in Section II we discuss the design and manufacturing process of a soft button array; in Section III we use the same technology to build a soft three-dimensional touchpad; finally, in Section IV we show how bend sensors can be connected to a compact processing unit that contains a smart vision camera and a microcontroller. All the code and data are available on `https://github.com/gaborsoter/phd_codes/tree/master/Skinflow`

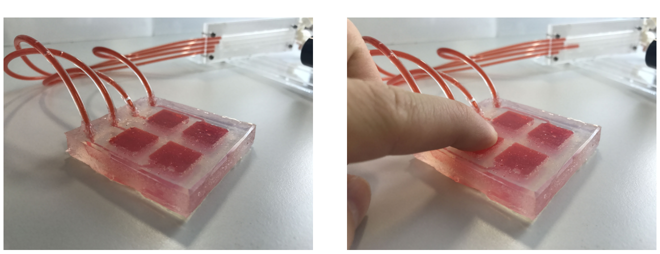

(a) (b)

Fig. 2: A soft sensor with four chambers filled with coloured liquid. By pressing the top surface of the chamber the volume change is transmitted to the display, where it is captured by the CCD camera.

II. Soft Button Array

The button array sensor consists of four chambers in a soft elastic body filled with coloured water (see Figure 2). Each reservoir has a cuboid shape and is surrounded by five thick (approx. 4 mm) and one thin wall on the top (2 mm). Each chamber is connected to a display through individual flexible tubes with 2 mm inner diameter. When a normal force is applied to one of the chambers the thin walls deform and the volume of the chamber decreases. Due to the incompressibility of the water the liquid is displaced in the display and this is captured by a CCD camera. A simple image processing algorithm is able to measure the liquid displacement and to provide real-time sensor values.

A. Fabrication

The elastic body is made of Sorta Clear 12 silicone (Smooth-On) by casting. The fabrication process is shown in Figure 3. First, the negative mold of the sensor is 3D printed with an Objet Connex printer using Vero White hard material. After cleaning, the mold is treated with caustic soda (NaOH) for two hours in order to improve surface finish and

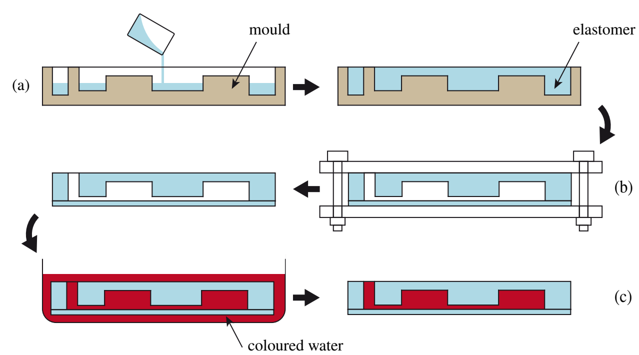

Fig. 3: Fabrication process. First, we create the top and bottom layers using silicone and 3D printed negative molds (a). Then, the two layers are glued together and placed in a mechanical press during curing (b). Finally, the sensors are filled with coloured water in a tank and attached to the flexible tubing (c).

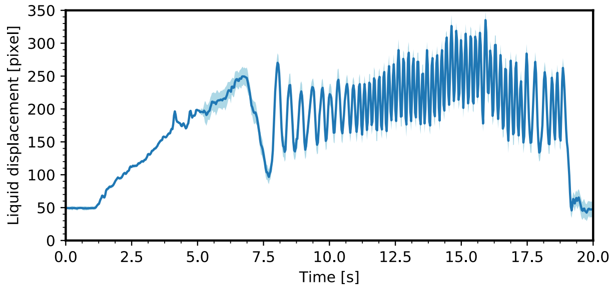

(a)

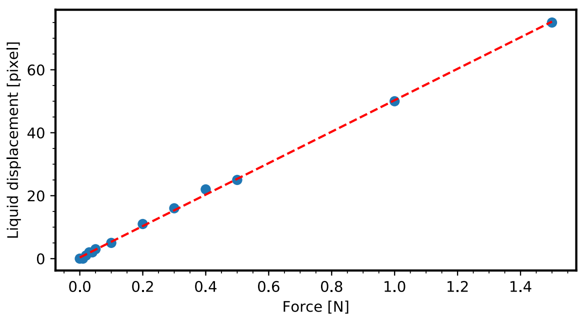

(b)

Fig. 4: Characteristics of a pressure sensitive soft button: (a) the response of the sensor to a slow hand push (before 7.5 s) and a fast vibration (after 7.5 s) shown with one standard deviation of measurement, (b) sensitivity of the soft button. The liquid displacement is defined as the difference between the actual and initial position of the coloured liquid in one channel.

to eliminate small amount of residue left on the surface. Next, the silicone is degassed in a vacuum chamber, poured into the mold and is placed in an oven of 40° C for 24 hours. The silicone cures with negligible shrinkage. After removing the cured elastic body from the mold, a 2 mm silicone layer is adhered to the bottom of the chambers to seal them. In order to improve the quality of bonding and to remove air bubbles from the uncured silicone we use a mechanical press during the curing process. After curing, the silicone body is placed in a tank filled with coloured tap water. By applying pressure to the chambers the air escapes from the chambers and channels, and upon relaxing the elastic material pulls the water inside. Finally, we remove the sensor from the tank and attach the flexible tubes that are connected to the display.

B. *Image processing*

The image processing algorithm is implemented on a personal computer and is written in Python using the OpenCV library. First, all the channels are individually cropped from the camera image. Then, we transform these images to greyscale and apply a threshold filter. The resolution of the camera is set to 640×420 and is placed 110 mm from the rigid display. In order to make the algorithm robust against noise we further divide each image into 9 subimages. The subimages' height is one pixel and their width is the horizontal resolution of the camera. Then we apply OpenCV's `countNonZero()` function on each subimages to count the number of non black pixels. And finally, we calculate the mean of these 9 values and use it as the sensor value.

C. *Characterisation*

The characterisation of the sensor is shown in Figure 4. The highest frequency that the sensor can measure is 30 Hz as the frame rate of the particular camera we used is 30 frames per second. It is important to note that both ends of the tubes are closed: on one end it is because of the design of the closed sensor chambers, while the other end is closed by plastic caps. This stops the fluids leaking from the channels and ensures return of the fluid after releasing force from the sensor. This enables the measurement of high frequency (>2 Hz) vibrations. Furthermore, we noticed that the water breaks up in the display cell (bubbles are introduced) if a very short high force impulse is applied and the closed ends help keep the water to be more cohesive. Although most silicones have nonlinear stress-strain response, the sensors presented in this work do not undergo large deformation. Due to geometric and design constrains (e.g. thin walls) the sensors have linear characteristics.

III. Three-dimensional soft touchpad

In this section we present the design, fabrication and analysis of a three-dimensional soft touchpad (see Figure 5),

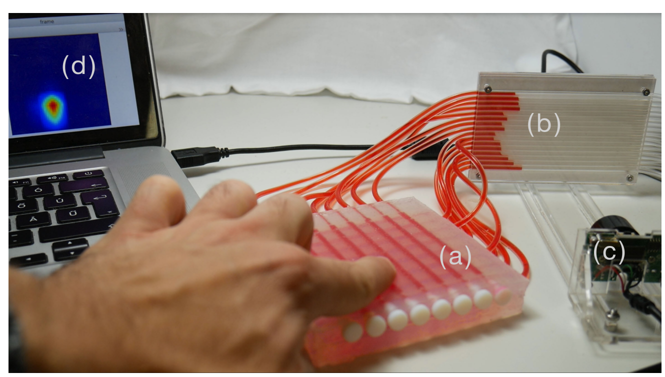

Fig. 5: The experimental setup that includes the (a) three-dimensional soft touchpad, (b) the display, (c) the CCD camera and (d) a computer for visualisation. By touching the surface of the device the image processing algorithm is able to detect the position and intensity of the touch in real-time. The user can interact with the device by deforming the soft surface.

which is able to sense the position as well as the intensity of a single touch. The touchpad is a stack of two identical layers, oriented at 90° compared to each other. Both layers have eight 80 mm long channels with 3 mm inner diameter. Each channel ends with a plastic cap on one side and with a tube on the other side. As the filling strategy presented in the previous section sometimes results in poor quality (e.g. small air bubbles in the liquid), we designed channels that can be opened and closed from both directions. This way the channels can be filled one-by-one using a syringe from one end. When the end of the liquid reached the desired point in the display, we close the other end of the tube. This stops the coloured water moving in the channels after removing the syringe. Finally, we close the other end with 3D printed end stops. Note that it is difficult to set all the liquid levels to the same position. However, with a simple calibration at the start the algorithm is able to deal with that without any problems.

A. *Fabrication*

Most of the fabrication process is identical to the process presented in the previous section, so here we detail only the differences. The shape of the 3D printed molds represents half of the internal structure of one layer. As these devices need to be sealed tightly, we used rectangular ridges between the channels. For each stacking process we used a mechanical press in order to remove bubbles.

B. *Algorithms*

As it is difficult to set the fluid levels to the same position in each channel the process starts with calibration. We collect data for the first 60 images (2 seconds), calculate the arithmetic mean of the time series for each channel and use this scalar as zero point. Then, we calculate the difference δ of the actual position of each channel and its zero point for each frame. These values are placed in two arrays δ_x and δ_y depending on which layer they belong to. Then, we discretise the two-dimensional image and apply first order linear interpolation in order to calculate the individual pixel values $p(x, y)$. During the discretisation process we needed to find an optimal value: too small discretisation results in low resolution measurement, while a too fine mesh slows down the image processing algorithm and increases the time delay between the physical interaction and the visualisation. In our case using 50 × 50 = 2500 nodes resulted in relatively good image quality and unnoticeable time delay. In order to make the algorithm robust against noise, $p(x, y)$ is calculated by the activation function

$$p(x, y) = 255 \cdot e^{c(\delta_x^n - 1)} \cdot e^{c(\delta_y^n - 1)}. \quad (1)$$

where $c = 5$ is a scalar that controls the sensitivity of the algorithm, δ_x^n and δ_y^n are the normalised values of the interpolated liquid displacements. The product of two exponential functions ensures that small oscillations are not detected. Finally, the image is recoloured using OpenCV's `COLORMAP_JET` colour scheme.

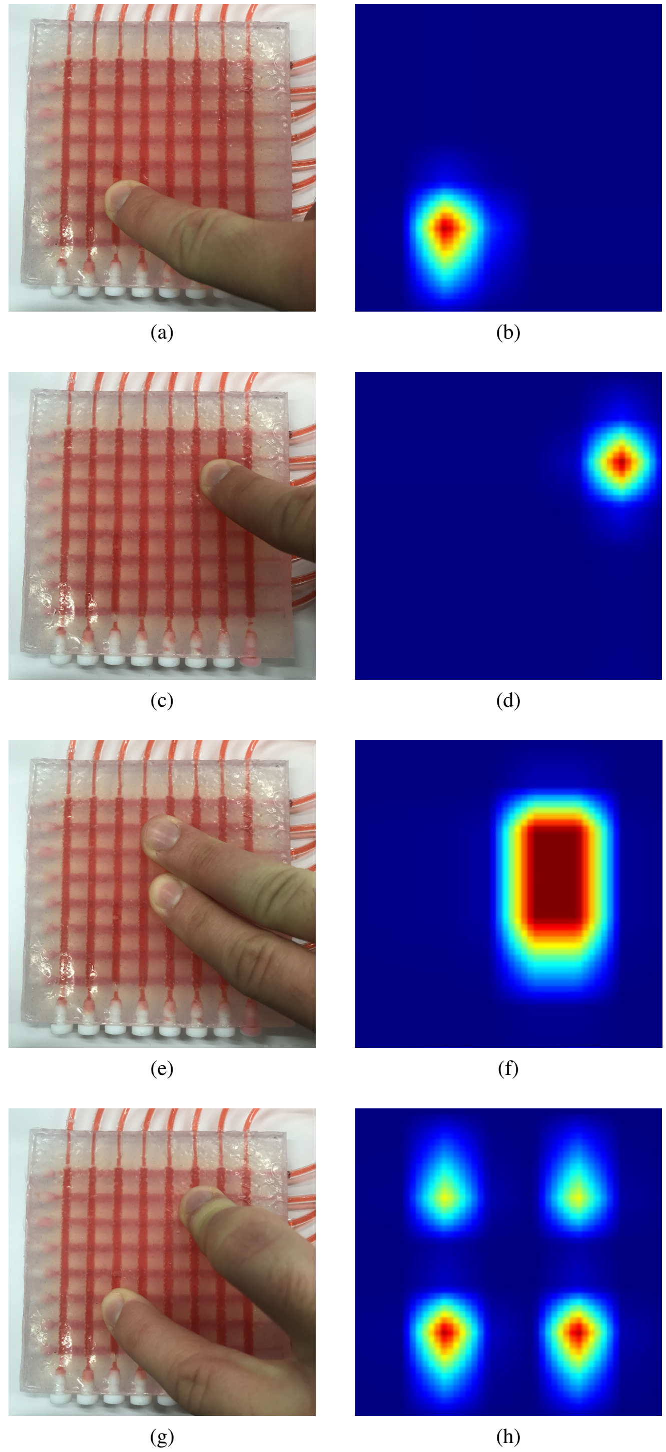

Fig. 6: The results of the image processing algorithm: (a-d) are examples for single touch: the localisation method is robust in case of one contact point. It can identify the position of the user's finger and it also provides information on the intensity of the touch. Different multi-touch scenarios are shown in (e-h). While two strong touches next to each other are sensed as one bigger touch (e, f), two contact points far from each other introduce the ghost touch effect. This is a common problem for resistive and capacitive touch screens (g, h).

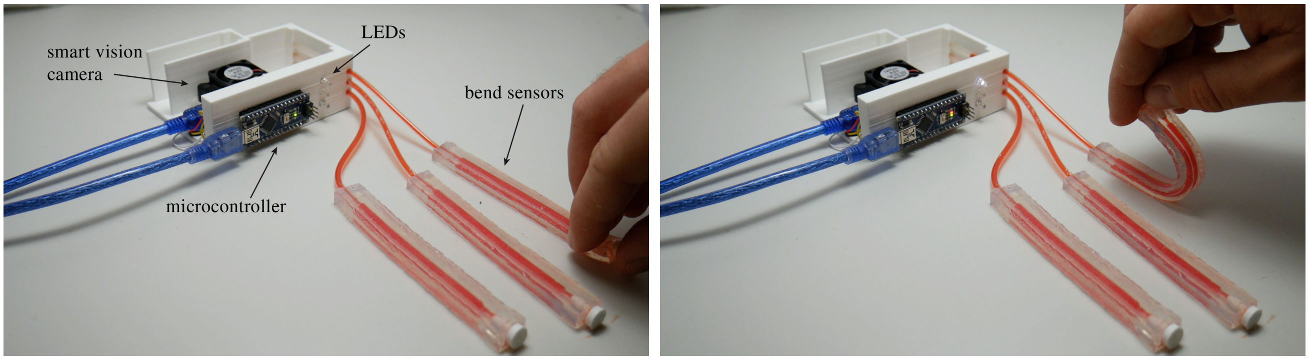

(a)

(b)

Fig. 7: Bend sensors connected to the processing unit. The device consists of a JeVois smart vision camera and an Arduino Nano microcontroller. When the sensors are bent the camera detects the fluid displacement and sends real-time data to the microcontroller using serial communication. Individual LEDs light up using a PWM signal according to the position of the fluid.

As can be seen in Figure 6 (a-d) the algorithm is able to find the accurate position of the contact point between a single finger and the soft touchpad. However, multiple simultaneous touches are not differentiated: two close touches result in one big rectangular blob (e, f) and two (or multiple) far touches cause the so-called ghost touch problem (g, h). One solution for the first problem is to increase the resolution of the device by reducing the diameter of the channels and increasing their number. This way the constant c in Equation 1 can be reduced and this would cause the increase of resolution in the direction of depth. In the case of the ghost touch problem, traditional solutions that were effective for previous touchscreens [23] cannot be used (e.g. voltage sensing) simply because the transduction mechanism is different. In our case this could be the solved by adding a third diagonal layer to the stack or by changing the geometry of the macrochannels.

IV. Bend sensors with compact design

The third device aims to demonstrate that a personal computer is not required to process the video captured by the camera: all the components can be integrated in a compact unit for autonomous real-time measurement. The setup includes three bend sensors and a processing unit which consists of a JeVois smart vision camera, an Arduino Nano microcontroller and three LEDs. Both the Arduino and the JeVois camera are connected to the same power bank. When liquid in the channels move due to bending of the sensors, the smart vision camera processes the information and controls the brightness of the LEDs through a microcontroller using pulse width modulation (PWM) signals (see Figure 7).

A. Fabrication

Most of the fabrication steps are identical to the previous sensors. Each sensor is 10 mm wide, 100 mm long and 5 mm thick. The case for electronics is 3D printed using a Wanhao type 3D printer using PLA filament. The microcontroller is connected to the smart vision camera using its 4-pin serial cable and they communicate on a 5V logic level with 115200 baud rate. The resolution of the camera is set to 320×240.

B. Algorithms

As in the previous cases, the image processing starts with colour filtering and greyscaling. Here we use three subimages with the height of one pixel for each channel and we average the number of non-black pixels. Then these values are sent to the microcontroller using serial communication.

The nonlinear behaviour of the sensor is shown in Figure 8. In our case the maximum liquid displacement is 126 pixels - almost the half of the image. The liquid displacement values were mapped to the [0, 255] range and were sent to the microcontroller.

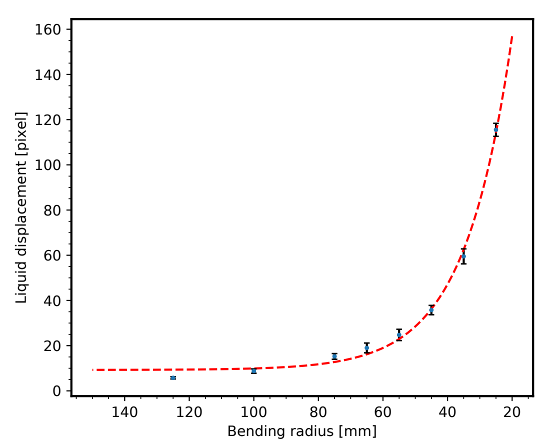

Fig. 8: Characteristics of the bend sensor with polynomial fit (shown with one standard deviation of measurement, we repeated the measurements five times for each data point).

V. Conclusions

In this paper we present a novel concept that combines soft, liquid filled and optical soft sensors. The sensors have two main parts: an entirely soft component that can be deformed by mechanical interactions such as pressure, bending and vibration, and a processing unit that includes a display and a CCD camera. When deforming the soft component the macrochannels embedded in the elastic body undergo volume change and a displacement of the liquid occurs in the channel. This change is captured by a CCD camera and can be quantified by real-time image processing algorithms. The proposed method allows us to create safe, scalable and stretchable sensors. The design and fabrication techniques of three different implementations were discussed. First, we created a pressure sensitive button array that contained chambers filled with coloured liquid. The sensor has high sensitivity and is able to measure vibrations up to 30 Hz. The second implementation was a three-dimensional touchpad. The soft component of the device included two identical layers oriented at 90° to each other with each layer contained eight closed channels. By measuring the displacement of the liquid in the channels we were able to calculate the position and the intensity of a single touch real-time. The device could be extended to measure multi-touch by increasing the resolution of the device (e.g. increasing the number of channels) or by adding a third diagonal layer. The third implementation showed how the devices required for real-time processing can be integrated in one compact design. Three bend sensors were connected to a rigid case and by bending them we changed the brightness of three LEDs using a smart vision camera and a microcontroller.

We have demonstrated the feasibility and usability of the proposed approach, but they can be still improved in many different ways. For example, using advanced manufacturing methods (e.g. ESCARGOT [24], soft lithography) it would be possible to create microchannels that have complicated, three-dimensional shapes. Another improvement could be to use the camera for more complex tasks as it can measure multiple channels as well as two-dimensional information. We will also investigate how the geometry and the connections of the channels can be changed in order to be able to perform computation, such as summation or edge detection, within the physical body.

REFERENCES

[1] B. Shih, J. Mayeda, Z. Huo, C. Christianson, and M. T. Tolley. 3D printed resistive soft sensors. In *2018 IEEE International Conference on Soft Robotics (RoboSoft)*, pages 152–157, April 2018.

[2] A. Atalay, V. Sanchez, O. Atalay, D. M. Vogt, F. Haufe, R. J. Wood, and C. J. Walsh. Batch fabrication of customizable silicone-textile composite capacitive strain sensors for human motion tracking. *Advanced Materials Technologies*, 2(9):1700136.

[3] Andreas T. and I. A. Anderson. A numerical method for measuring capacitive soft sensors through one channel. *Smart Materials and Structures*, 27(3):035016, 2018.

[4] M. Luo, E. H. Skorina, W. Tao, F. Chen, S. Ozel, Y. Sun, and C. D. Onal. Toward modular soft robotics: Proprioceptive curvature sensing and sliding-mode control of soft bidirectional bending modules. *Soft Robotics*, 4(2):117–125, 2017. PMID: 29182091.

[5] Y. Park, B. Chen, and R. J. Wood. Design and fabrication of soft artificial skin using embedded microchannels and liquid conductors. *IEEE Sensors Journal*, 12(8):2711–2718, Aug 2012.

[6] B. Ward-Cherrier, N. Pestell, L. Cramphorn, B. Winstone, M. E. Giannaccini, J. Rossiter, and N. F. Lepora. The tactip family: Soft optical tactile sensors with 3d-printed biomimetic morphologies. *Soft Robotics*, 5(2):216–227, 2018. PMID: 29297773.

[7] R. Scharff, R. Doornbusch, A. Klootwijk, A. Doshi, Z. Doubrovski, J. Wu, J. Geraedts, and C. Wang. Color-based sensing of bending deformation on soft robots. In *IEEE International Conference on Robotics and Automation (ICRA)*, 2018.

[8] M. D. Dickey. Stretchable and soft electronics using liquid metals. *Advanced Materials*, 29(27):1606425.

[9] M. Kim, H. Alrowais, C. Kim, and O. Brand. All-soft sensing platform based on liquid metal for liquid- and gas-phase voc detection. In *2016 IEEE SENSORS*, pages 1–3, Oct 2016.

[10] L. Zhou, Q. Gao, J. Zhan, C. Xie, J. Fu, and Y. He. Three-dimensional printed wearable sensors with liquid metals for detecting the pose of snakelike soft robots. *ACS Applied Materials & Interfaces*, 10(27):23208–23217, 2018. PMID: 29911853.

[11] M. Kim, C. Kim, H. Alrowais, and O. Brand. Multiscale and uniform liquid metal thin-film patterning based on soft lithography for 3d heterogeneous integrated soft microsystems: Additive stamping and subtractive reverse stamping. *Advanced Materials Technologies*, 3(7):1800061.

[12] M. D. Dickey. Stretchable and soft electronics using liquid metals. *Advanced Materials*, 29(27):1606425.

[13] K. Noda, E. Iwase, K. Matsumoto, and I. Shimoyama. Stretchable liquid tactile sensor for robot-joints. In *2010 IEEE International Conference on Robotics and Automation*, pages 4212–4217, May 2010.

[14] J. Chossat, Y. Tao, V. Duchaine, and Y. Park. Wearable soft artificial skin for hand motion detection with embedded microfluidic strain sensing. In *2015 IEEE International Conference on Robotics and Automation (ICRA)*, pages 2568–2573, May 2015.

[15] T. Helps and J. Rossiter. Proprioceptive flexible fluidic actuators using conductive working fluids. *Soft Robotics*, 5(2):175–189, Apr 2018. 29211627[pmid].

[16] L. Fujun, Y. Yongze, and L. Jing. Transformations of liquid metals in ionic liquid. *arXiv:1704.03742 [physics.flu-dyn]*, 2017.

[17] L. Jiang, K. Low, J. Costa, R. J. Black, and Y. Park. Fiber optically sensorized multi-fingered robotic hand. In *2015 IEEE/RSJ International Conference on Intelligent Robots and Systems (IROS)*, pages 1763–1768, Sept 2015.

[18] C. To, T. L. Hellebrekers, and Y. Park. Highly stretchable optical sensors for pressure, strain, and curvature measurement. In *2015 IEEE/RSJ International Conference on Intelligent Robots and Systems (IROS)*, pages 5898–5903, Sept 2015.

[19] C. Chorley, C. Melhuish, T. Pipe, and J. Rossiter. Development of a tactile sensor based on biologically inspired edge encoding. In *2009 International Conference on Advanced Robotics*, pages 1–6, June 2009.

[20] B. Winstone, G. Griffiths, T. Pipe, C. Melhuish, and J. Rossiter. *TACTIP - Tactile Fingertip Device, Texture Analysis through Optical Tracking of Skin Features*, pages 323–334. Springer Berlin Heidelberg, Berlin, Heidelberg, 2013.

[21] G. Soter, A. Conn, H. Hauser, N. F. Lepora, and J. Rossiter. Multitip: A multimodal mechano-thermal soft fingertip. In *2018 IEEE International Conference on Soft Robotics (RoboSoft)*, pages 239–244, April 2018.

[22] S. Landkammer, R. Valek, and R. Hornfeck. A novel bio-inspired fluidic actuator for robotic applications. *International Conference on Adaptive Structures and Technologies (ICAST)*, 2014.

[23] P. Coni, J. Nol Perbet, Y. Sontag, and J. Christophe Abadie. 31.2: Eliminating ghost touches on a self-capacitive touch-screen. *SID Symposium Digest of Technical Papers*, 43, 06 2012.

[24] V. Saggiomo and A. H. Velders. Simple 3D printed scaffold-removal method for the fabrication of intricate microfluidic devices. *Advanced Science*, 2(9):1500125.